

# Photoelectron Spectroscopy Studies of the Electronic Structures of Al/RbF and Al/CaF<sub>2</sub> Cathodes for Alq<sub>3</sub>-based Organic Light-emitting Devices

Yongsup Park<sup>\*a</sup> and Jouhahn Lee<sup>\*b</sup>

## Abstract

The electronic structures of Al/RbF/*tris*-(8-hydroxyquinoline)aluminium (Alq<sub>3</sub>) and Al/CaF<sub>2</sub>/Alq<sub>3</sub> interfaces were investigated using x-ray photoelectron spectroscopy (XPS) and ultraviolet photoelectron spectroscopy (UPS). For both systems, the UPS showed a significant valence band shift following the deposition of the thin fluoride layers on Alq<sub>3</sub>. However, the formation of gap state in valence region and the extra peak N 1s core level spectra showed different trends, suggesting that the alkali fluoride and alkali-earth fluoride interlayer have different reaction mechanisms at the interface between Al cathode and Alq<sub>3</sub>. In addition, the deposition of Al has considerably less effect on the valence band shift compared to the deposition of both RbF and CaF<sub>2</sub>. These results suggest that the charge transfer across the interface and the resulting gap state formation may have lesser effect on the enhancement of organic light-emitting device performance than the observed valence band shift, which is thought to lower the electron injection barrier.

**Keywords** : OLED, electron injection layer, photoelectron spectroscopy, energy level alignment

## 1. Introduction

The organic light-emitting devices (OLED) have been attracting a lot of attentions with respect to their applications on flat panel display. A typical OLED has a cathode made of a low work function metal (LWFM) for the electron injection and a transparent anode made of a high work function indium-tin-oxide (ITO) coated glass for the hole injection. Recombination of injected electrons and holes in the emission layer produces electroluminescence [1]. Thin film of *tris*-(8-hydroxyquinoline)aluminum (Alq<sub>3</sub>) is one of the most widely used materials for OLEDs due to its excellent stability and luminescent properties [1, 2, 3]. In addition, Alq<sub>3</sub> shows high potential toward the emitting material for large area display [4]. Many efforts have been made to improve the performance of OLEDs. One of the major OLED performance improvement was made by inserting an insulating thin layer between the metal cathode

and the light-emitting material layer [5, 6, 7]. The insertion of a thin LiF interlayer between the Alq<sub>3</sub> layer and a metal cathode has shown dramatic performance improvement of OLEDs [8]. However, the nature of this performance improvement resulting from the sandwiched interlayer has not yet been fully understood, despite the few suggestions have been reported. Tunnelling through a metal fluoride layer was proposed by Hung *et al* [8]. Then the formation of a dipole layer across the interface leading to a vacuum level offset between the organic layer and the Al cathode was initially proposed by Shaheen *et al.* [9], and recently by Brabec *et al.* as a means to enhance performance [10]. Then, dissociation of the LiF and doping mechanism of the organic layer was proposed by Le *et al* [6]. However the physics behind these phenomena is still not clear [11].

In this report, we investigated the effect of thin RbF and CaF<sub>2</sub> interlayers between the Alq<sub>3</sub> layer and an Al cathode layer using x-ray photoelectron spectroscopy (XPS) and ultraviolet photoelectron spectroscopy (UPS). The shift of highest occupied molecular orbital (HOMO) level to higher binding energy side was clearly observed as a result of both RbF and CaF<sub>2</sub> deposition. In case of Al/RbF cathode, the appearance of an extra peak in the N 1s core level spectra accompanied by the formation of the gap states resembles the case of Al/LiF cathode. However, for

Manuscript received January 12, 2005; accepted for publication March 25, 2005.

\* Member, KIDS.

Corresponding Author : Yongsup Park

a. Nano-Surface Group, Korea Research Institute of Standards and Science, P.O. Box 102Yuseong, Daejeon 305 -600, Korea.

b. Korea Basic Science Institute, Jeonju Center, Jeonju 561-756, Korea.

E-mail : park@kriss.re.kr Tel : +42 868-5397 Fax : +42 868-5032

Al/CaF<sub>2</sub> cathode, the interface electronic structure showed a different behavior from those found in Al/LiF/Alq<sub>3</sub> and Al/RbF/Alq<sub>3</sub> interfaces. It is much more similar to those observed in Al/MgF<sub>2</sub>/Alq<sub>3</sub> structure which was previously reported [12, 13].

## 2. Experiments

The XPS and UPS experiments were carried out in an ultrahigh vacuum analysis chamber that is connected to a preparation chamber where all deposition processes took place *in situ*. Spectra were recorded on VG ESCALAB 220 using a He I (21.2 eV) radiation source for UPS and a Mg K $\alpha$  (1253.6 eV) radiation for XPS. The base pressure of the preparation chamber and the analysis chamber were  $1 \times 10^{-9}$  and  $5 \times 10^{-10}$  Torr, respectively. UPS spectra were recorded with a bias of -20 V on the sample for the observation of the low energy cutoff. Energy resolutions were approximately 0.1 eV and 1.0 eV for UPS and XPS, respectively. A 10 nm thick Alq<sub>3</sub> film was initially deposited on ITO coated glass as a starting surface. The deposition of insulating metal fluoride on Alq<sub>3</sub>/ITO was carefully monitored by crystal quartz microbalance and the typical rate was 0.1~0.2 nm/min. The ultimate structure and thickness of the sample with were therefore set to Al (2 nm)/metal fluoride interlayer (0.5 nm)/Alq<sub>3</sub> (10 nm)/ITO (60 nm).

## 3. Results and Discussion

Fig. 1(a) show a series of valence band spectra of RbF/Alq<sub>3</sub> with increasing RbF thickness. This Fig. clearly shows the marked valence band shift caused by the RbF deposition on Alq<sub>3</sub> layer. The binding energy (BE) in Fig. 1 is relative to the Fermi level of spectra,  $E_F$ . The spectrum for a pristine Alq<sub>3</sub> layer is seen at the bottom. The onset of the peak at the lowest binding energy is the HOMO level and is attributed to the orbital located on the phenoxide side of the quinolate ligand. The HOMO level of Alq<sub>3</sub> is estimated to be 2.4 eV below the Fermi energy, which is in good agreement with the values previously reported [5, 12, 14]. With the deposition of RbF, the HOMO level can be seen to have shifted towards the higher BE. The HOMO level shift is about 1.2 eV at RbF coverage of 0.5 nm. In

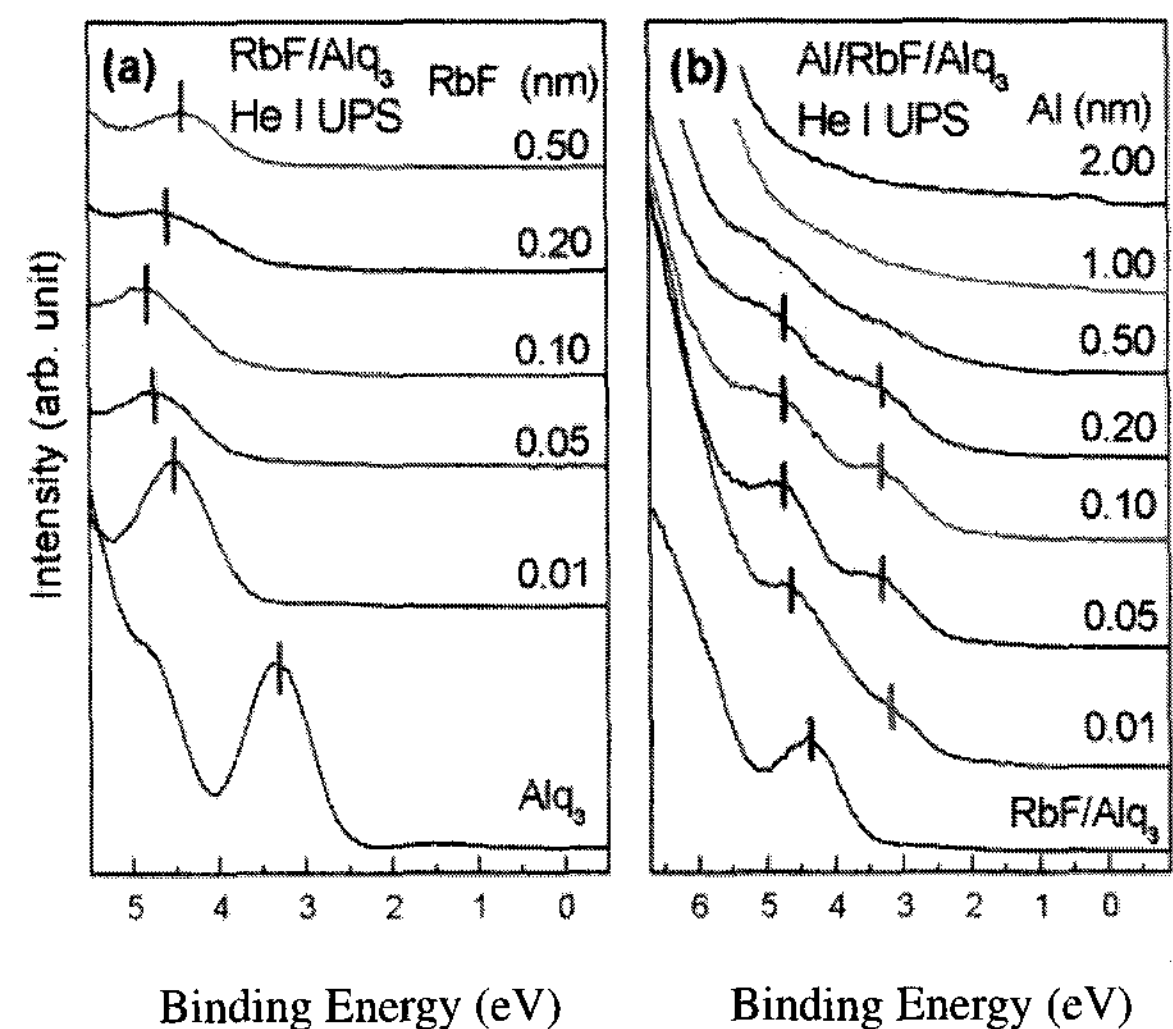


**Fig. 1.** (a) The evolution of the valence band spectra for RbF/Alq<sub>3</sub> with increasing RbF coverage. (b) Valence band spectra of Al deposition on RbF/Alq<sub>3</sub>. The gap states indicated by arrows can be clearly observed. The binding energy is relative to the Fermi level.

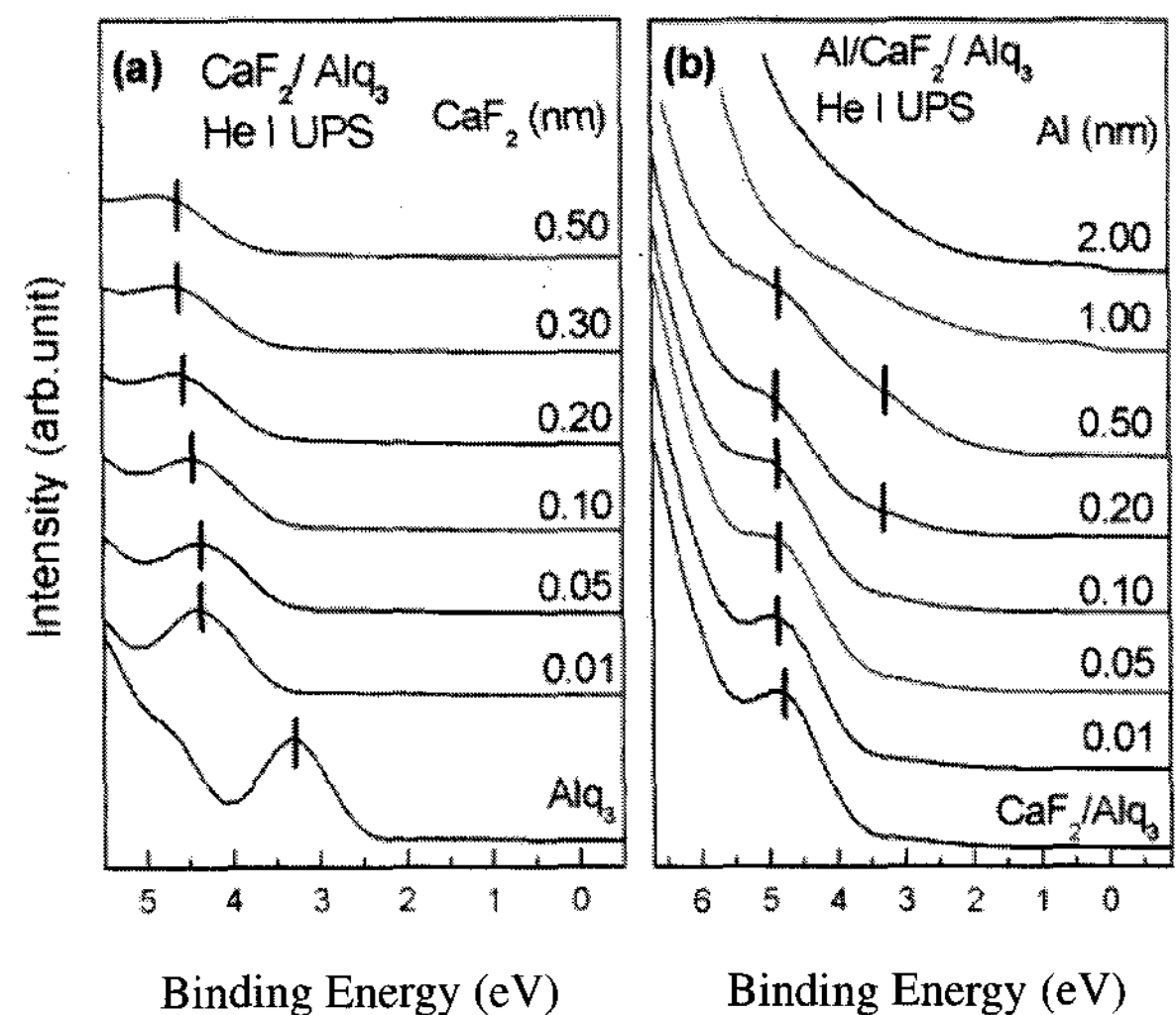


**Fig. 2.** (a) The evolution of the valence band spectra for CaF<sub>2</sub>/Alq<sub>3</sub> with increasing CaF<sub>2</sub> coverage. (b) Valence band spectra of Al deposition on CaF<sub>2</sub>/Alq<sub>3</sub>. The gap states indicated with arrows shows very weak feature.

Fig. 1(b), we can see the evolution of valence region spectra with increasing Al thickness on the RbF(0.5 nm)/Alq<sub>3</sub>(10 nm) system. The deposition of Al yields an extra peak at the lower BE side of HOMO level, indicated with second vertical bar, which is assigned to the gap state formation. The intensity is similar to the Al/LiF/Alq<sub>3</sub> interface.

Fig. 2 shows a series of valence band spectra of

Al/CaF<sub>2</sub>/Alq<sub>3</sub> system. In Fig. 2(a), the whole valence band shifted toward higher BE direction and the Alq<sub>3</sub> features were attenuated as a result of CaF<sub>2</sub> deposition. The amount of shift is about 1.5 eV at CaF<sub>2</sub> coverage of 0.5 nm. In Fig. 2(b), we can see the evolution of valence region spectra with increasing Al thickness on the CaF<sub>2</sub>(0.5 nm)/Alq<sub>3</sub>(10 nm). The deposition of Al also yields gap states formation which also occurred in case of Al/RbF/ Alq<sub>3</sub>. The formation of gap states indicated with a vertical bar is clearly observed, even though the intensity is much weaker than in Al/RbF/Alq<sub>3</sub> interface.

For both Al/RbF and Al/CaF<sub>2</sub> cathodes, a major shift occurred on initial metal fluorides deposition (0.01 nm), suggesting that the whole interlayer coverage on Alq<sub>3</sub> is not necessary to pull down the whole valence band including the HOMO. The deposition of Al did not cause the significant peak shift but did cause a gap state to develop, suggesting that the gap state formation is not playing a major role in pulling down the HOMO level. If the HOMO level shift by metal fluoride layer deposition represents a rigid shift of all the valence levels including the lowest unoccupied molecular orbital (LUMO), then the LUMO pull-down relative to  $E_F$  and resultant lower electron injection barrier can be understood as the main reason for the improved OLED performance [15].

Fig. 3 shows the evolution of XPS Al 2*p*, O 1*s*, N 1*s*, C 1*s*, F 1*s* and Rb 3*d* core level spectra for various Al coverages RbF/Alq<sub>3</sub>. In Fig. 3(a), the single peak at 74.3 eV in the bottom spectra is associated with Al atoms in pristine Alq<sub>3</sub>. When 0.5 nm of RbF was deposited, the Al 2*p* peak shifted 0.7 eV towards higher BE but the peak shape did not change. But when 0.1 nm of Al was deposited, the peak shifted by 0.3 eV to higher BE and was slightly broadened. No significant peak shift or broadening was observed even though Al was further deposited. From 0.5 nm Al coverage, a new peak at lower BE side started to appear. The presence of a strong peak at 72.8 eV with 2.0 nm aluminum coverage is attributed to the metallic Al. The appearance of strong metallic Al 2*p* peak at 2.0 nm of Al coverage coincides with the observation of the Fermi edge in the valence spectra shown in Fig. 1(b). The evolution of O 1*s* featured in Fig. 3(b) also shows a similar trend. The O 1*s* peak for the pristine Alq<sub>3</sub> appears at 531.6 eV. With the deposition of RbF, the O 1*s* peak shifted 0.4 eV to higher binding energy and was slightly broadened. The O 1*s* peak did not shift much when with further Al deposition but

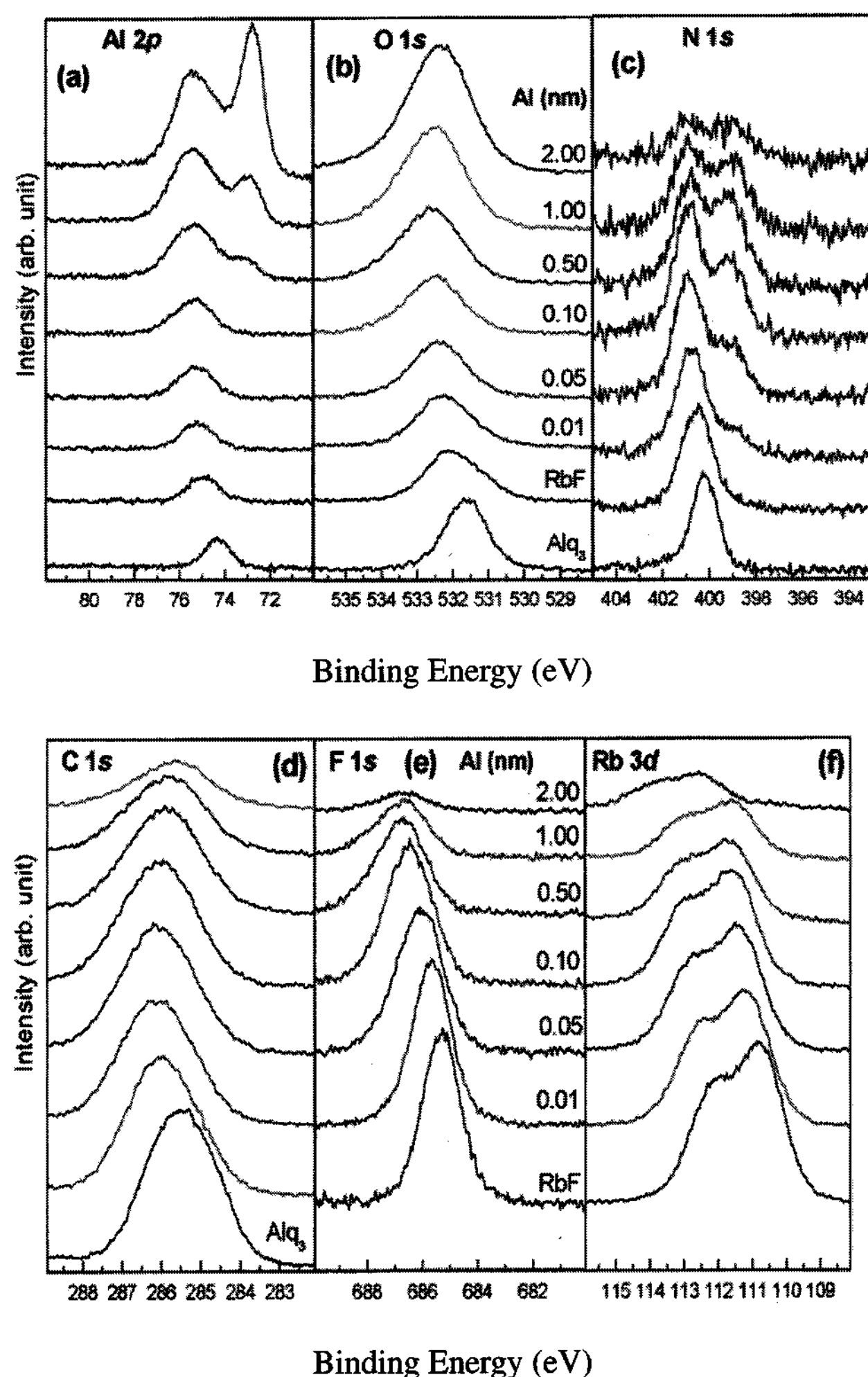
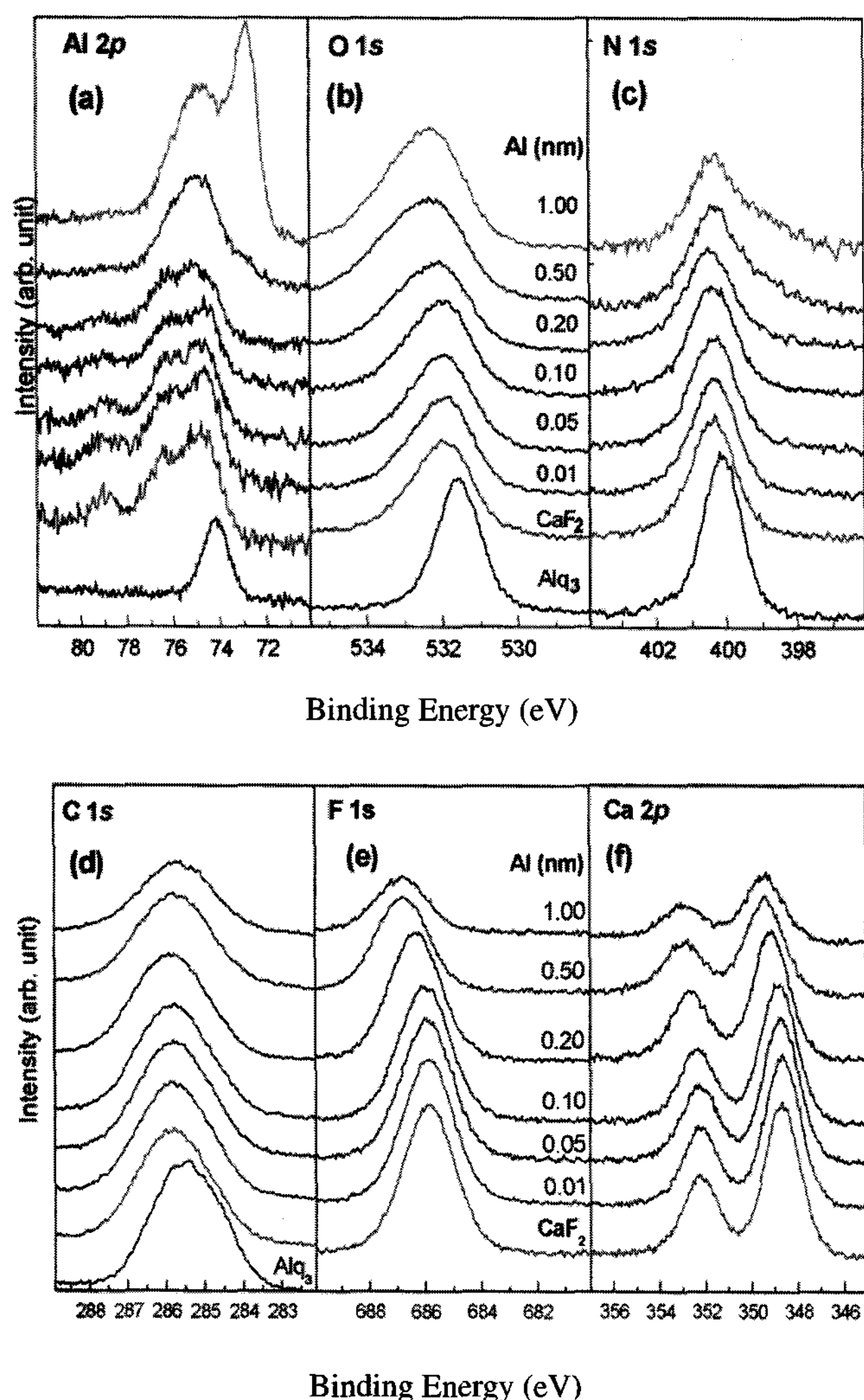


Fig. 3. (a) The evolution of XPS core level spectra of Al 2*p* peak with RbF and Al deposition. (b) Similar evolution of O 1*s*, (c) N 1*s*, (d) C 1*s*, (e) F 1*s*, and (f) Rb 3*d* peaks.

did show some broadening. This indicates that the broad peak probably from aluminum oxides dominates the spectrum as the features from Alq<sub>3</sub> and RbF deposition were buried under the thick aluminum and its oxide layer. In Fig. 3(c), the evolution of N 1*s* core level spectra shows the strong appearance of the shoulder peak on the lower BE side of the N 1*s* due to a charge transfer from the metal atoms. N 1*s* XPS spectra will be further discussed in a later section in comparison with Al/CaF<sub>2</sub> interface. The behavior of the C 1*s* peak was not significantly affected throughout the deposition processes except for a slight broadening of the peak. The Rb 3*d* and the F 1*s* peaks from deposited RbF also did not show any significant change upon deposition of Al on RbF/Alq<sub>3</sub>, except that both Rb 3*d* and F 1*s* peaks shifted slightly to higher BE direction.





**Fig. 4.** (a) XPS core level spectra of Al 2*p* peak with CaF<sub>2</sub> and Al deposition. (b) Similar evolution of O 1*s*, (c) N 1*s*, (d) C 1*s*, (e) F 1*s*, and (f) Ca 2*p* peaks. In (c), the extra peak in the lower BE shows considerably weak feature than Al/RbF/Alq<sub>3</sub> interface.

Fig. 4 shows the XPS core level spectra of Al/CaF<sub>2</sub>/Alq<sub>3</sub> interface. As seen in Fig. 4(a), the deposition of 0.5 nm CaF<sub>2</sub> yielded an extra peak in the higher BE side of Al 2*p* peak at about 1.6 eV from the main peak. This indicates that the chemical state of the Al atom in Alq<sub>3</sub> was altered by the deposition of CaF<sub>2</sub>. The deposition of Al on CaF<sub>2</sub>/Alq<sub>3</sub> creates initially only a single shoulder peak, even though the strong peaks at 72.8 eV and 74.9 eV, corresponding to the metallic Al and its oxide, respectively, eventually dominate at high Al coverage. Both O 1*s* core level peak and C 1*s* core level peak are similar to those observed in Al/RbF/Alq<sub>3</sub> system. Ca 2*p* core level peak and F 1*s* peaks shifted slightly to higher BE direction at Al coverage of 0.2

nm. The deposition of both CaF<sub>2</sub> on Alq<sub>3</sub> and Al on CaF<sub>2</sub>/Alq<sub>3</sub> did not seem to cause any significant change except for the slight peak position shift.

In 4(c), with 0.5 nm of Al coverage, a very weak shoulder in lower BE side of the N 1*s* core level peak was observed whereas Al/RbF/Alq<sub>3</sub> interface exhibited marked growths of the extra peak within the same region as seen in Fig. 4. The core level spectra of Al/CaF<sub>2</sub>/Alq<sub>3</sub> show similar trend as shown in our previous studies on Al/MgF<sub>2</sub>/Alq<sub>3</sub> [12]. It is well known according to the studies conducted on metal deposition on Alq<sub>3</sub> that the appearance of shoulder peak is accompanied by the formation of gap states in valence region in low BE side of the N 1*s* core level peak of Alq<sub>3</sub> due to a charge transfer from the metal atoms [13], [16]. However, Al/CaF<sub>2</sub>/Alq<sub>3</sub> interface shows different spectra trend from Al/RbF/Alq<sub>3</sub>. This suggests that there exists a different interface reaction mechanism between the alkali-metal fluoride interface and alkali-earth-metal fluoride interface in OLEDs. Both interfaces exhibited the formation of gap states as a result of Al deposition. Whether the extra peak in the N 1*s* core level spectra strong or weak, the enhancement of OLEDs performance for both CaF<sub>2</sub> and LiF interlayered interfaces was observed [13], indicating that the charge transfer mechanism at the interface has little effect on the OLED performance.

We have reported that the valence band shift, which is directly related with the enhancement of OLED performance through HOMO level shift, results from the metal fluoride deposition rather than from the gap state formation accompanied by the appearance of extra peak in N 1*s* core level spectra [13]. The origin of the gap states and N 1*s* shoulder peak still remains speculative at this stage. It might be due to charge transfer from Ca after CaF<sub>2</sub> is dissociated. Another possible explanation is that the Al deposited on CaF<sub>2</sub>/Alq<sub>3</sub> might still find the bare Alq<sub>3</sub> surface and partially form Al/Alq<sub>3</sub> interface. It was shown in our previous work that Al/Alq<sub>3</sub> interface exhibited weak extra peak at lower BE of N 1*s* main peak [13]. The origin of the peak shift due to the metal fluorides deposition is still not fully understood. Therefore we speculate that the pinning of the Fermi level due to some kind of chemical reaction between the interlayer and Alq<sub>3</sub> might be the cause of the observed valence band shifts.

#### 4. Summary

The interface electronic structures of Al/RbF/Alq<sub>3</sub> and Al/CaF<sub>2</sub>/Alq<sub>3</sub> were investigated using XPS and UPS in the context of OLED performance enhancement. The valence band shift occurred when both metal fluorides were deposited even before Al deposition. This shift is considered to lower the electron injection barrier by pulling down the LUMO level. The deposition of Al on RbF/Alq<sub>3</sub> formed stronger gap states and markedly evolving shoulder feature in N 1s compared to considerably weaker peak feature that appeared in Al/CaF<sub>2</sub>/Alq<sub>3</sub> interface. These results support the different behavior of Al/alkali-earth metal fluoride/Alq<sub>3</sub> interface from Al/alkali metal fluoride/Alq<sub>3</sub> and other LWFM/Alq<sub>3</sub> interfaces. These similarity and difference between the two interlayers suggest that the complex charge transfer mechanism across the interface which is the origin of the gap states may have considerably lesser effect on the enhancement of OLED performance than the valence band shift caused by the deposition of interlayer fluorides.

#### References

- [ 1 ] C. W. Tang and S. A. VanSlyke, *Appl. Phys. Lett.*, **51**, 913 (1987).
- [ 2 ] C. W. Tang, S. A. VanSlyke, and C. H. Chen, *J. Appl. Phys.*, **65**, 3610 (1989).
- [ 3 ] S. A. VanSlyke, C. H. Chen, and C. W. Tang, *Appl. Phys. Lett.*, **69**, 2160 (1996).
- [ 4 ] T. Mori, H. Fujikawa, S. Tokito, and Y. Taga, *Appl. Phys. Lett.*, **73**, 2763 (1998).
- [ 5 ] Q. T. Le, L. Yan, Y. Gao, M. G. Mason, D. J. Giesen, and C. W. Tang, *J. Appl. Phys.*, **87**, 375 (2000).
- [ 6 ] P. Piromreun, H. Oh, Y. Shen, G. G. Malliaras, J. C. Scott, and P. J. Brock, *Appl. Phys. Lett.*, **77**, 2403 (2000).
- [ 7 ] L. S. Hung, C. W. Tang, and M. G. Mason, *Appl. Phys. Lett.*, **70**, 152 (1997).
- [ 8 ] S. E. Shaheen, G. E. Jabbour, M. M. Morell, Y. Kawabe, B. Kippelen, N. Peyghambarian, M. F. Nabor, R. Shlaf, E. A. Mash, and N. R. Armstrong, *J. Appl. Phys.*, **84**, 2324 (1998).
- [ 9 ] C. J. Brabec, S. E. Shaheen, C. Winder, and N. S. Sariciftci, *Appl. Phys. Lett.*, **80**, 1288 (2002).
- [ 10 ] T. M. Brown, R. H. Friend, I. S. Millard, D. J. Lacey, J. H. Burroughes, and F. Cacialli, *Appl. Phys. Lett.*, **79**, 174 (2001).
- [ 11 ] Y. Park, J. Lee, S. K. Lee, and D. Y. Kim, *Appl. Phys. Lett.*, **79**, 105 (2001).
- [ 12 ] J. Lee, Y. Park, S. K. Lee, E.-J. Cho, D. Y. Kim, H. Y. Chu, H. Lee, L.-M. Do, and T. Zyung, *Appl. Phys. Lett.*, **80**, 3123 (2002).
- [ 13 ] D. Y. Kim, S. Cho, and Y. Park, *J. Korean Phys. Soc.*, **37**, 598 (2000).
- [ 14 ] R. Schlaf, B. A. Parkinson, P. A. Lee, K. W. Nebesny, G. Jabbour, B. Kippelen, N. Peyghambarian, and N. R. Armstrong, *J. Appl. Phys.*, **84**, 6729 (1998).
- [ 15 ] M. G. Mason, C. W. Tang, L.-S. Hung, P. Raychaudhuri, J. Madathil, D. J. Giesen, L. Yan, Q. T. Le, Y. Gao, S.-T. Lee, L. S. Liao, L. F. Cheng, W. R. Salaneck, D. A. dos Santos, and J. L. Bredas, *J. Appl. Phys.*, **89**, 2756 (2001).